EUV and Soft X-Ray Beamlines

David Attwood
University of California, Berkeley

Cheiron School
September 2011
SPring-8

Beamlines are used to transport photons to the sample, and take a desired spectral slice

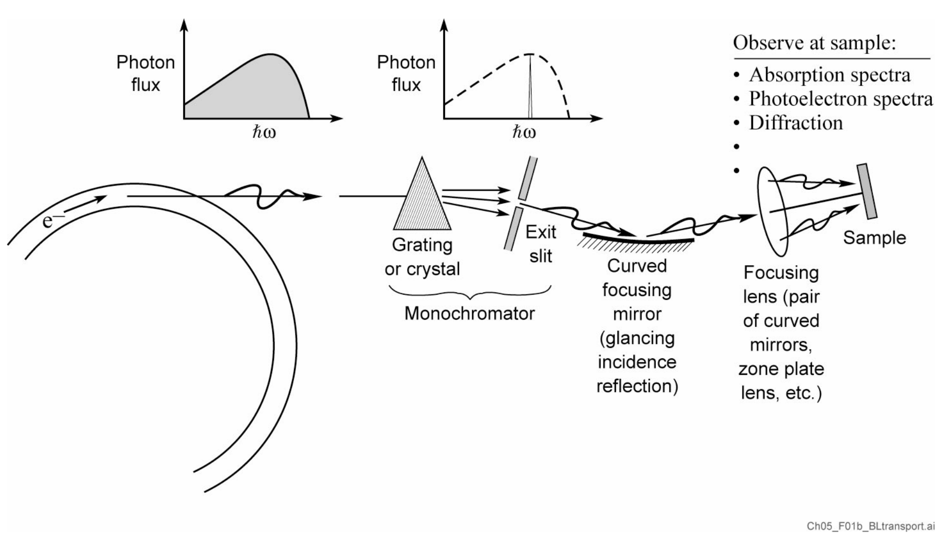

A typical beamline: monochromator plus focusing optics to deliver radiation to the sample

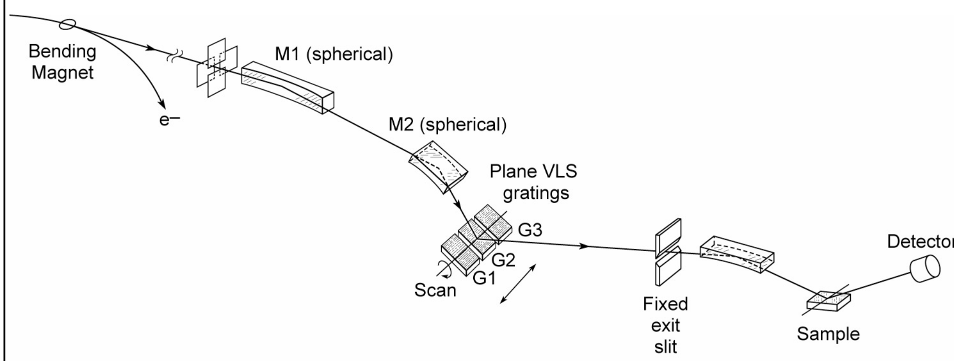

Courtesy of James Underwood (EUV Technology Inc.)

Beamline 7.0 at Berkeley's Advanced Light Source

Undulator radiated power in the central cone

$$\lambda_x = \frac{\lambda_u}{2\gamma^2}\left(1 + \frac{K^2}{2} + \gamma^2\theta^2\right)$$

$$\bar{P}_{cen} = \frac{\pi e \gamma^2 I}{\epsilon_0 \lambda_u} \frac{K^2}{(1 + \frac{K^2}{2})^2} f(K)$$

$$\theta_{cen} = \frac{1}{\gamma^* \sqrt{N}}$$

$$\left(\frac{\Delta\lambda}{\lambda}\right)_{cen} = \frac{1}{N}$$

$$K = \frac{e B_0 \lambda_u}{2\pi m_0 c}$$

$$\gamma^* = \gamma / \sqrt{1 + \frac{K^2}{2}}$$

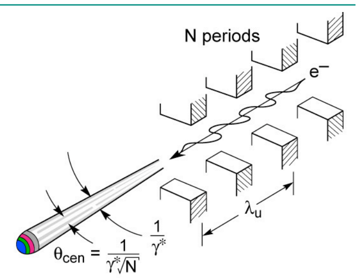

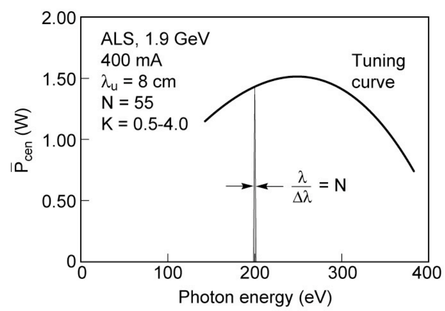

Power in the central radiation cone for three x-ray undulators

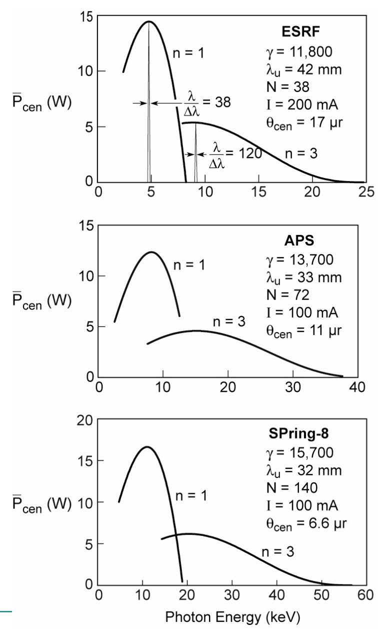

$$\theta_{cen} = \frac{1}{\gamma^* \sqrt{N}}$$

$$\left[\frac{\Delta\lambda}{\lambda}\right]_1 = \frac{1}{N}$$

$$\left[\frac{\Delta\lambda}{\lambda}\right]_3 = \frac{1}{3N}$$

High spectral resolution (meV beamline)

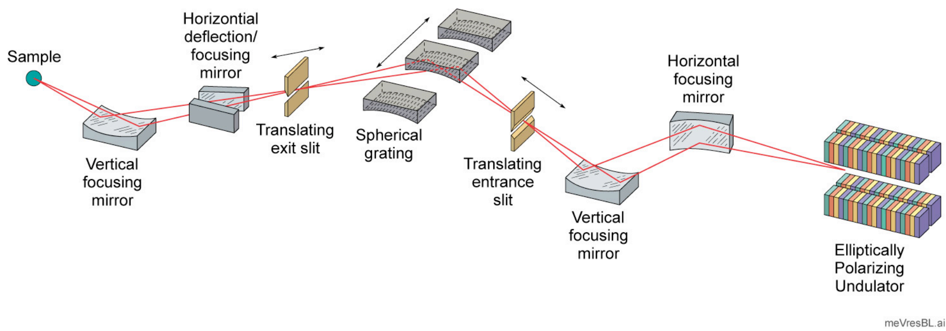

Courtesy of Zahid Hussein (ALS)

MAESTRO: A new varied-line-space grating monochromator beam line for angle-resolved-photo-electron-spectroscopy with high spectral and spatial resolution at the Advanced Light Source

Jason Wells, Derek Yegian, Ken Chow, Eli Rotenberg, Aaron Bostwick, Geoff Gaines and Tony Warwick

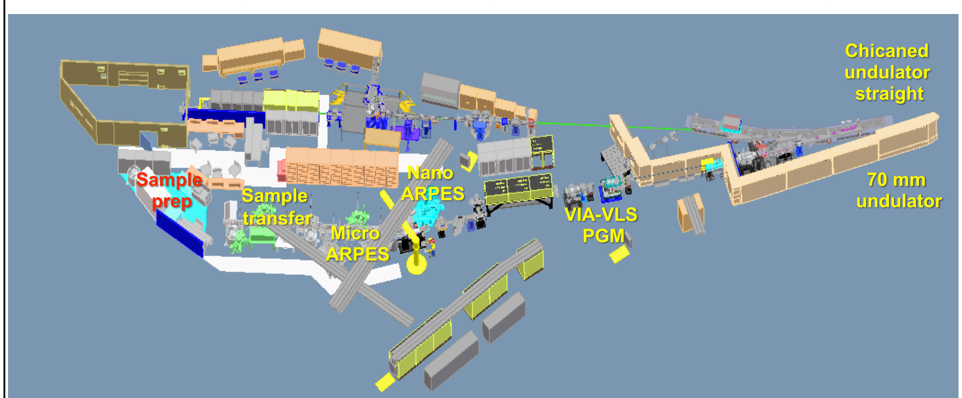

The latest soft x-ray undulator spectroscopy beam line planned for the ALS serves **MAESTRO** a new high resolution Angle Resolved Photo Emission facility with zone-plate focused nano-ARPES. The beam line design offers spectral resolution 1:30000 from 60eV to 400eV with an extended energy range from 20eV to 1000eV. Challenges include optical figure quality, thermal engineering, source size and stability and vibrations in the monochromator. The optical design is radical in that a VLS grating will provide all of the focusing in the dispersion direction, and the mirrors are plane, except for a sphere to collect and focus horizontally.

Courtesy of Eli Rotenberg and Tony Warwick (ALS)

Varied line space gratings

Varied-Line-Space Plane Gratings provide focusing and aberration correction along with the dispersion that they generate in the monochromator. They can be used to erect the monochromator focal plane, making the position of the focus at the exit slit (almost) stationary as the grating rotates to select the photon energy. Beyond that, they are now being used to replace the focusing from shaped optics, making beam lines cheaper and easier to align.

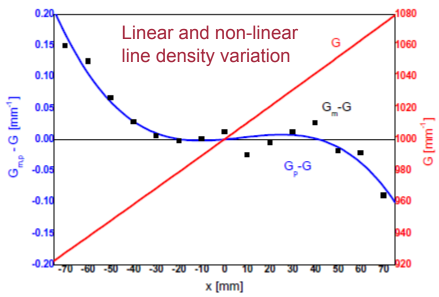

The PEEM3 beam line at 11.0.2 uses a Triple-Ruled Varied-Line-Space grating:

1) to erect the focal plane on a stationary set of exit slits
2) to keep the zero-order light in focus, for easy tuning, and for monitoring of the photon energy.

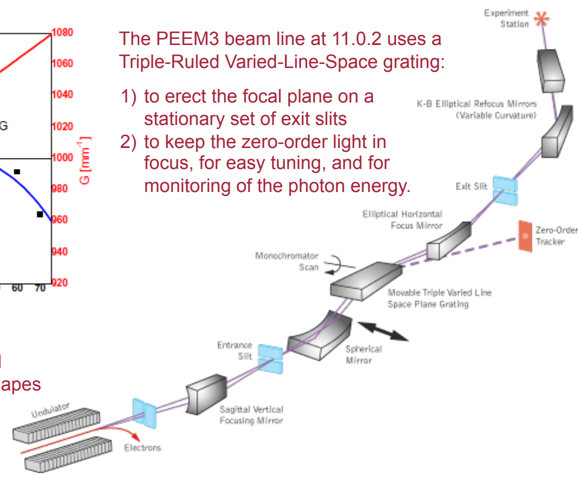

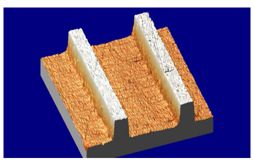

AFM measured groove shapes

Courtesy of Tony Warwick (ALS) CheironSchool_Oct2010_Lec2.ppt 9

MAESTRO: A new varied-line-space grating monochromator beam line at the ALS

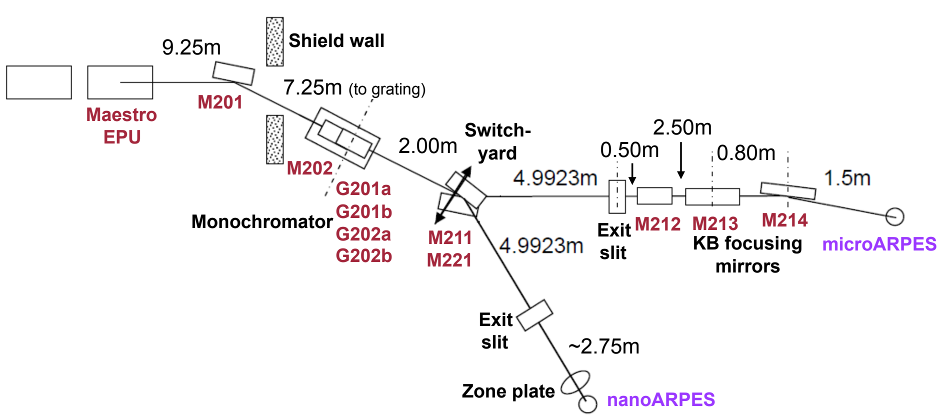

Courtesy of Tony Warwick (ALS) CheironSchool_Oct2010_Lec2.ppt 10

MAESTRO at the ALS: gratings and efficiencies

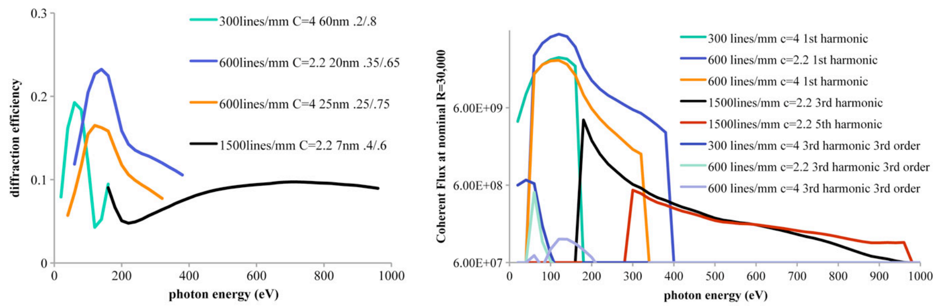

Courtesy of Tony Warwick (ALS)

CheironSchool_Oct2010_Lec2.ppt 11

Water-cooled optics are essential: correcting slope errors due to a thermal bump

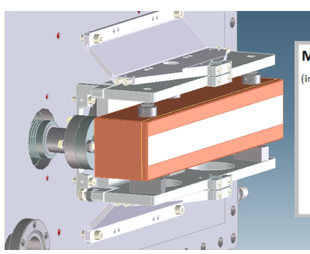

M201 Plane - Slope Errors (μRad)	over full mirror substrate		over clear aperture	
(internally cooled Glidcop, 10K W/m²K)	60eV	20eV	60eV	20eV
Maximum Tangential Slope Error	28.2	61.3	28.2	61.3
Average Tangential Slope Error	2.4	4.9	3.0	6.1
RMS Tangential Slope Error	3.3	7.0	4.4	9.3
Maximum Sagittal Slope Error	36.4	75.1	36.4	75.1
Average Sagittal Slope Error	7.3	15.3	13.9	29.2
RMS Sagittal Slope Error	12.2	25.6	18.0	38.0

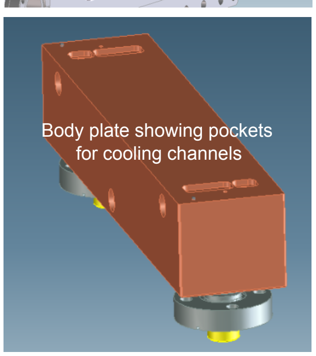

Height error

Tangential slope error

Sagittal slope error

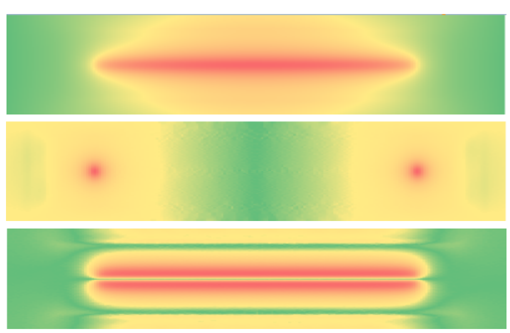

Courtesy of Tony Warwick (ALS)

CheironSchool_Oct2010_Lec2.ppt 12

Ray tracing beamlines is an important tool

Significant degradation of the spectral resolution occurs due to localized heating of M202. It is almost entirely corrected by adjusting the monochromator focusing parameter from 3.93 to 4.02. The engineering design will allow this mirror to be built with 1mm thick hot-wall and the actual thermal deformation is expected to be less.

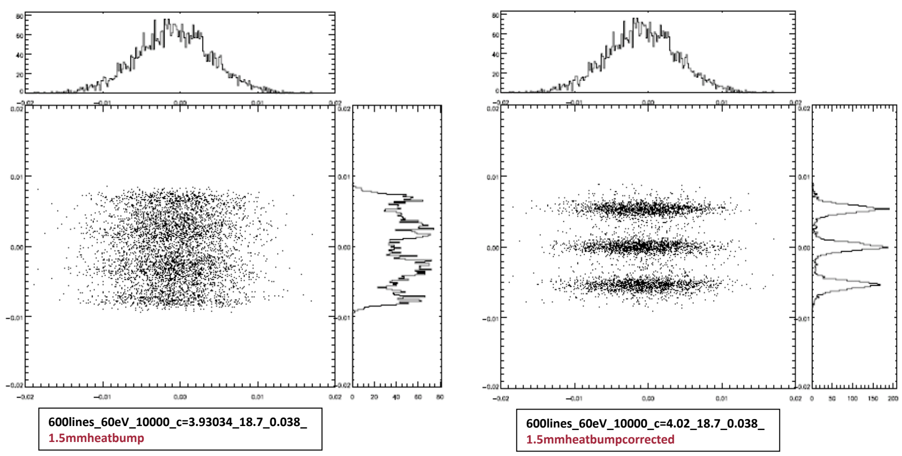

Courtesy of Tony Warwick (ALS) CheironSchool_Oct2010_Lec2.ppt 13

References

Reininger, R., Kriesel, K., Hulbert, S.L., Sanchez-Hanke, C. and Arena, D.A., Rev. Sci. Instrum.,79, 033108 2008

Peterson, H., Jung, C., Hellwig, C. Peatman, W.B. and Gudat, W., Rev. Sci. Instrum. 66 (1995) 1

Follath, R., and Senf, F., Nucl.Intrum. Methods Phys. Res. A390 (1997) 388

Amemiya, K., Kitajima, Y.,Ohta, T., and Ito, K., J. Synchrotron Radiation 3 (1996) 282

The original SHADOW package is available at www.nanotech.wisc.edu/CNTLABS/shadow.html and with an IDL user interface at www.esrf.fr/computing/scientific/xop

Undulator Radiation, Ellaume, P., in Undulators, Wigglers and their Applications,

Onuki, H. and Ellaume, P. eds., Taylor and Francis.

Characteristics of Synchrotron Radiation, Kim, K., J., in Xray Data Booklet LBNL internal report (1986) PUB 490 xdb.lbl.gov/xdb.pdf

D Fluckiger - Grating Solver Development Company Dec 2006 www.gsolver.com

Courtesy of Tony Warwick (ALS) CheironSchool_Oct2010_Lec2.ppt 14

Typical parameters for synchrotron radiation

Facility	ALS	New Subaru	APS	SP-8
Electron energy	1.90 GeV	1.00 GeV	7.00 GeV	8.00 GeV
γ	3720	1957	13,700	15,700
Current (mA)	400	100	100	100
Circumference (m)	197	119	1100	1440
RF frequency (MHz)	500	500	352	509
Pulse duration (FWHM) (ps)	35-70	26	100	120
Bending Magnet Radiation:				
Bending magnet field (T)	1.27	1.03	0.599	0.679
Critical photon energy (keV)	3.05	0.685	19.5	28.9
Critical photon wavelength	0.407 nm	1.81 nm	0.636 Å	0.429 Å
Bending magnet sources	24	4	35	23
Undulator Radiation:				
Number of straight sections	12	4	40	48
Undulator period (typical) (cm)	5.00	5.40	3.30	3.20
Number of periods	89	200	72	140
Photon energy ($K = 1$, $n = 1$)	457 eV	117 eV	9.40 keV	12.7 keV
Photon wavelength ($K = 1$, $n = 1$)	2.71 nm	10.6 nm	1.32 Å	0.979 Å
Tuning range ($n = 1$)	230-620 eV	43-170 eV	3.5-12 keV	4.7-19 keV
Tuning range ($n = 3$)	690-1800 eV	130-500 eV	10-38 keV	16-51 keV
Central cone half-angle ($K = 1$)	35 μrad	44 μrad	11 μrad	6.6 μrad
Power in central cone ($K = 1$, $n = 1$) (W)	2.3	0.15	12	16
Flux in central cone (photons/s)	3.1×10^{16}	7.9×10^{15}	7.9×10^{15}	7.9×10^{15}
σ_x, σ_y (μm)	260, 16	450, 220	320, 50	380, 6.8
σ'_x, σ'_y (μrad)	23, 3.9	89, 18	23, 7	16, 1.8
Brightness ($K = 1$, $n = 1$)[a] [(photons/s)/mm^2 · mrad^2 · (0.1%BW)]	2.3×10^{19}	1.7×10^{17}	5.9×10^{18}	1.8×10^{20}
Total power ($K = 1$, all n, all θ) (W)	83	27	350	2,000
Other undulator periods (cm)	3.65, 8.00, 10.0	7.60	2.70, 5.50, 12.8	2.4, 10.0, 3.7, 12.0
Wiggler Radiation:				
Wiggler period (typical) (cm)	16.0		8.5	12.0
Number of periods	19		28	37
Magnetic field (maximum) (T)	2.1		1.0	1.0
K (maximum)	32		7.9	11
Critical photon energy (keV)	5.1		33	43
Critical photon wavelength	0.24 nm		0.38 Å	0.29 Å
Total power (max. K) (kW)	13		7.4	18

[a] Using Eq. (5.65). See comments following Eq. (5.64) for the case where $\sigma'_{x,y} \simeq \theta_{cen}$.

Ch05_T1b_VG_Nov05.ai ol_Sept2011_Lec2.ppt

15

Time structure of synchrotron radiation

The axial electric field within the RF cavity, used to replenish lost (radiated) energy, forms a potential well "bucket" system that forces electrons into axial electron "bunches". This leads to a time structure in the emitted radiation.

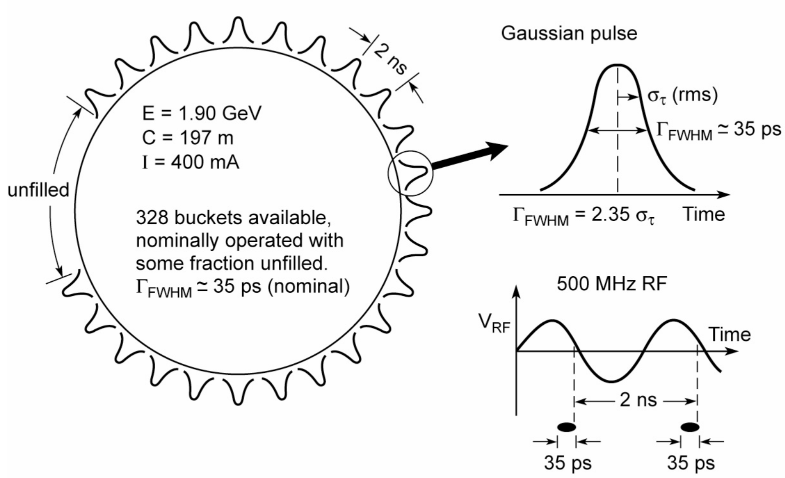

Ch05_TimeStruc.ai

16

CheironSchool_Sept2011_Lec2.ppt

Beamlines for spatially coherent undulator radiation

λ = 11.2 nm

λ = 13.4 nm

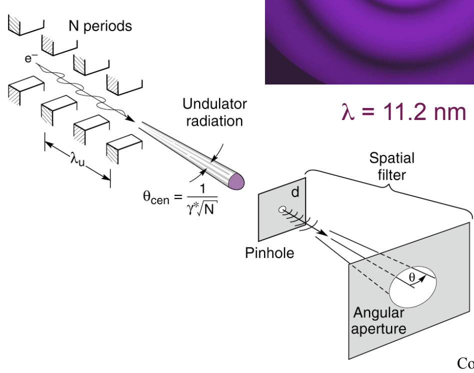

1 μm^D pinhole

25 mm wide CCD at 410 mm

Courtesy of Patrick Naulleau, LBNL.

17
CheironSchool_Sept2011_Lec2.ppt

Coherence at short wavelengths

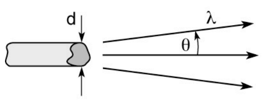

$l_{coh} = \lambda^2/2\Delta\lambda$ {temporal (longitudinal) coherence} (8.3)

$d \cdot \theta = \lambda/2\pi$ {spatial (transverse) coherence} (8.5)

or $d \cdot 2\theta|_{FWHM} = 0.44\,\lambda$ (8.5*)

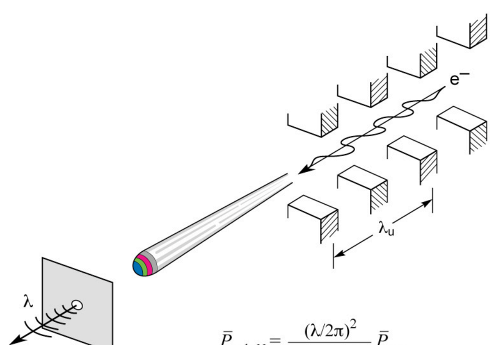

$$\bar{P}_{coh,N} = \frac{(\lambda/2\pi)^2}{(d_x\theta_x)(d_y\theta_y)}\bar{P}_{cen} \quad (8.6)$$

$$\bar{P}_{coh,\lambda/\Delta\lambda} = \frac{e\lambda_u I\eta(\Delta\lambda/\lambda)N^2}{8\pi\epsilon_0 d_x d_y} \cdot \left[1 - \frac{\hbar\omega}{\hbar\omega_0}\right] f(K) \quad (8.9)$$

Ch08_F00_Sept2010.ai

18
CheironSchool_Sept2011_Lec2.ppt

Young’s double slit experiment: spatial coherence and the persistence of fringes

Persistence of fringes as the source grows
from a point source to finite size.

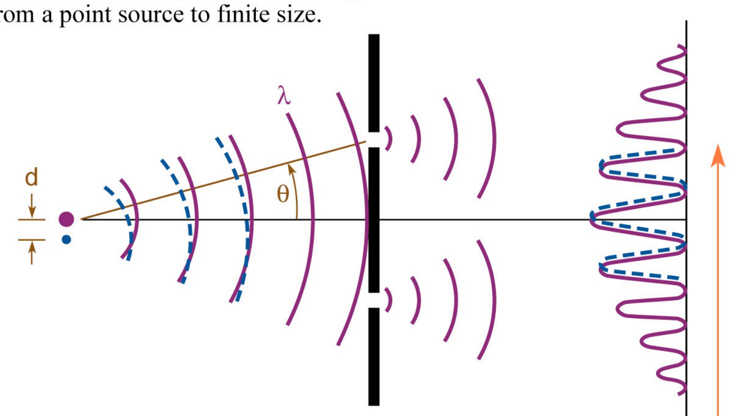

$$d \cdot 2\theta|_{FWHM} \simeq \lambda/2$$

$$\lambda_{coh} = \lambda^2/2\Delta\lambda = \frac{1}{2} N_{coh}\lambda$$

CH08_YoungsExprmt_v3.ai

19
CheironSchool_Sept2011_Lec2.ppt

Spatial and spectral filtering to produce coherent radiation

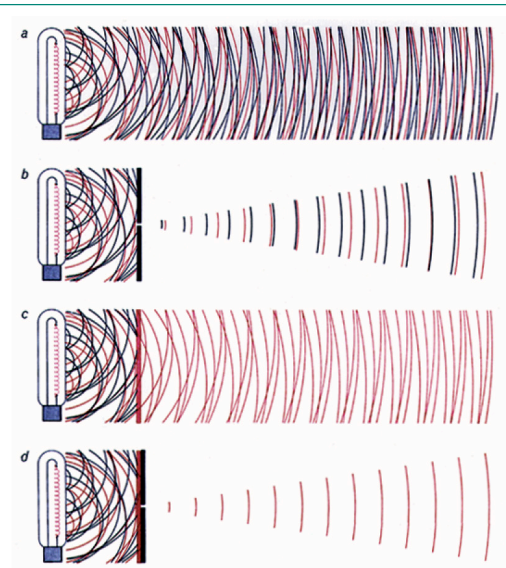

Courtesy of A. Schawlow, Stanford.

Ch08_F08.ai

20
CheironSchool_Sept2011_Lec2.ppt

Spatial and temporal coherence

Mutual coherence factor

$$\Gamma_{12}(\tau) \equiv \langle E_1(t+\tau)E_2^*(t)\rangle \qquad (8.1)$$

Normalize degree of spatial coherence (complex coherence factor)

$$\mu_{12} = \frac{\langle E_1(t)E_2^*(t)\rangle}{\sqrt{\langle|E_1|^2\rangle}\sqrt{\langle|E_2|^2\rangle}} \qquad (8.12)$$

A high degree of coherence ($\mu \to 1$) implies an ability to form a high contrast interference (fringe) pattern. A low degree of coherence ($\mu \to 0$) implies an absence of interference, except with great care. In general radiation is partially coherent.

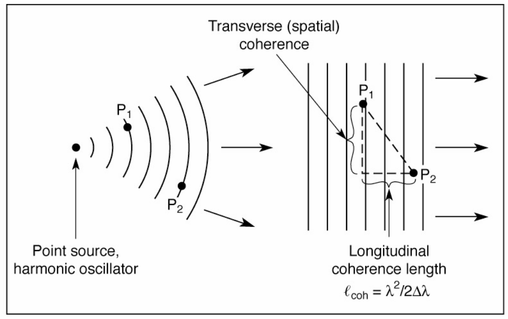

Longitudinal (temporal) coherence length

$$\ell_{coh} = \frac{\lambda^2}{2\,\Delta\lambda} \qquad (8.3)$$

Full spatial (transverse) coherence

$$d \cdot \theta = \lambda/2\pi \qquad (8.5)$$

Ch08_Eq1_12_F2.ai

Spatially filtered undulator radiation

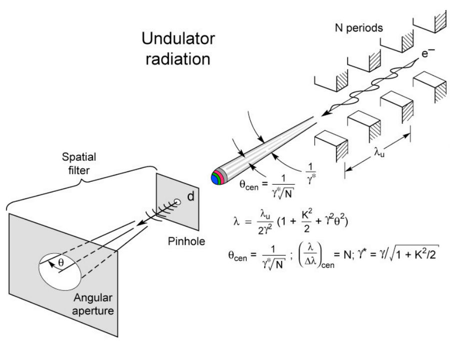

Using a pinhole-aperture spatial filter, passing only radiation that satisfies $d \cdot \theta = \lambda/2\pi$

$$\bar{P}_{coh,N} = \left(\frac{\lambda/2\pi}{d_x\theta_x}\right)\left(\frac{\lambda/2\pi}{d_y\theta_y}\right)\bar{P}_{cen} \qquad (8.6)$$

$$\bar{P}_{coh,N} = \frac{e\lambda_u IN}{8\pi\epsilon_0 d_x d_y}\left(1 - \frac{\hbar\omega}{\hbar\omega_0}\right) f(\hbar\omega/\hbar\omega_0) \qquad (8.9)$$

for $d_x = 2\sigma_x$, $d_y = 2\sigma_y$, $\theta_{Tx} \to \theta_x$, $\theta_{Ty} \to \theta_y$, and $\sigma'^2 << \theta^2_{cen}$.

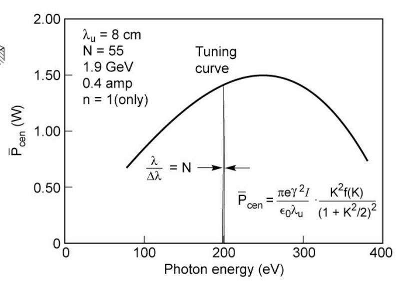

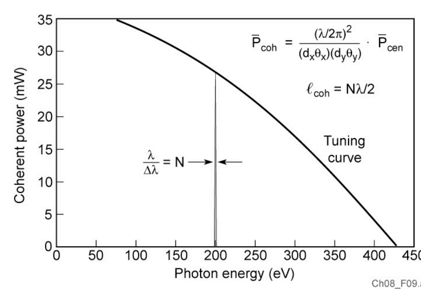

Ch08_F09.ai

Spatial and spectral filtering of undulator radiation

In addition to the pinhole – angular aperture for spatial filtering and spatial coherence, add a monochromator for narrowed bandwidth and increased temporal coherence:

$$\bar{P}_{\text{coh},\lambda/\Delta\lambda} = \underbrace{\eta}_{\substack{\text{beamline}\\ \text{efficiency}}} \underbrace{\frac{(\lambda/2\pi)^2}{(d_x\theta_x)(d_y,\theta_y)}}_{\substack{\text{spatial}\\ \text{filtering}}} \cdot \underbrace{N\frac{\Delta\lambda}{\lambda}}_{\substack{\text{spectral}\\ \text{filtering}}} \cdot \bar{P}_{\text{cen}} \qquad (8.10a)$$

which for $\sigma'^2_{x,y} << \theta^2_{cen}$ (the undulator condition) gives the spatially and temporally coherent power ($d \cdot \theta = \lambda/2\pi$; $l_{\text{coh}} = \dfrac{\lambda^2}{2\,\Delta\lambda}$)

$$\bar{P}_{\text{coh},\lambda/\Delta\lambda} = \frac{e\lambda_u I\eta(\Delta\lambda/\lambda)N^2}{8\pi\epsilon_0 d_x d_y} \cdot \left(1 - \frac{\hbar\omega}{\hbar\omega_0}\right) f(\hbar\omega/\hbar\omega_0) \qquad (8.10c)$$

which we note scales as N^2.

Ch08_SpatialSpectral.ai

CheironSchool_Sept2011_Lec2.ppt 23

Spatially and spectrally filtered undulator radiation

- Pinhole filtering for full spatial coherence
- Monochromator for spectral filtering to $\lambda/\Delta\lambda > N$

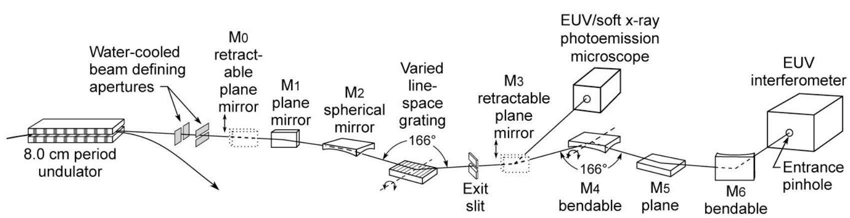

$$\bar{P}_{\text{coh},\lambda/\Delta\lambda} = \underbrace{\eta}_{\substack{\text{beamline}\\ \text{efficiency}}} \underbrace{\frac{(\lambda/2\pi)^2}{(d_x\theta_x)(d_y\theta_y)}}_{\substack{\text{spatial}\\ \text{filtering}}} \cdot \underbrace{N\frac{\Delta\lambda}{\lambda}}_{\substack{\text{spectral}\\ \text{filtering}}} \cdot \bar{P}_{\text{cen}} \qquad (8.10a)$$

$$\bar{P}_{\text{coh},\lambda/\Delta\lambda} = \frac{e\lambda_u I\eta(\Delta\lambda/\lambda)N^2}{8\pi\epsilon_0 d_x d_y} \cdot \left(1 - \frac{\hbar\omega}{\hbar\omega_0}\right) f(\hbar\omega/\hbar\omega_0)$$

$$(\sigma'^2 \ll \theta^2_{\text{cen}}) \qquad (8.10c)$$

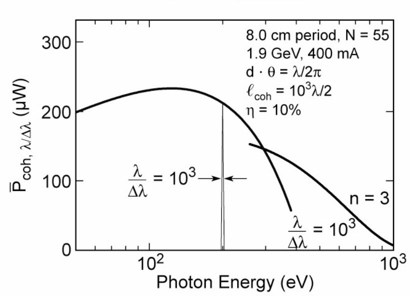

Ch08_F11_Mar08.ai

CheironSchool_Sept2011_Lec2.ppt 24

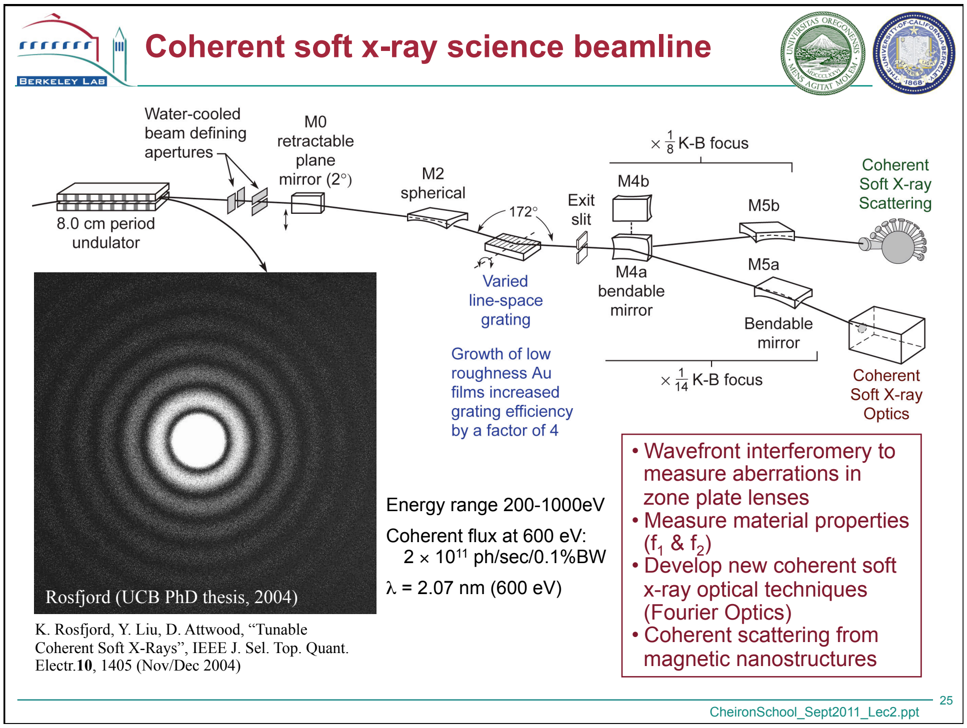
BERKELEY LAB
Coherent soft x-ray science beamline
Water-cooled beam defining apertures
M0 retractable plane mirror (2°)
M2 spherical
172°
Exit slit
× 1/8 K-B focus
M4b
M5b
Coherent Soft X-ray Scattering
8.0 cm period undulator
Varied line-space grating
M4a bendable mirror
M5a
Bendable mirror
Coherent Soft X-ray Optics
× 1/14 K-B focus
Growth of low roughness Au films increased grating efficiency by a factor of 4
Rosfjord (UCB PhD thesis, 2004)
K. Rosfjord, Y. Liu, D. Attwood, "Tunable Coherent Soft X-Rays", IEEE J. Sel. Top. Quant. Electr.10, 1405 (Nov/Dec 2004)
Energy range 200-1000eV
Coherent flux at 600 eV: 2×10^{11} ph/sec/0.1%BW
λ = 2.07 nm (600 eV)
• Wavefront interferometry to measure aberrations in zone plate lenses
• Measure material properties (f_1 & f_2)
• Develop new coherent soft x-ray optical techniques (Fourier Optics)
• Coherent scattering from magnetic nanostructures
25
CheironSchool_Sept2011_Lec2.ppt

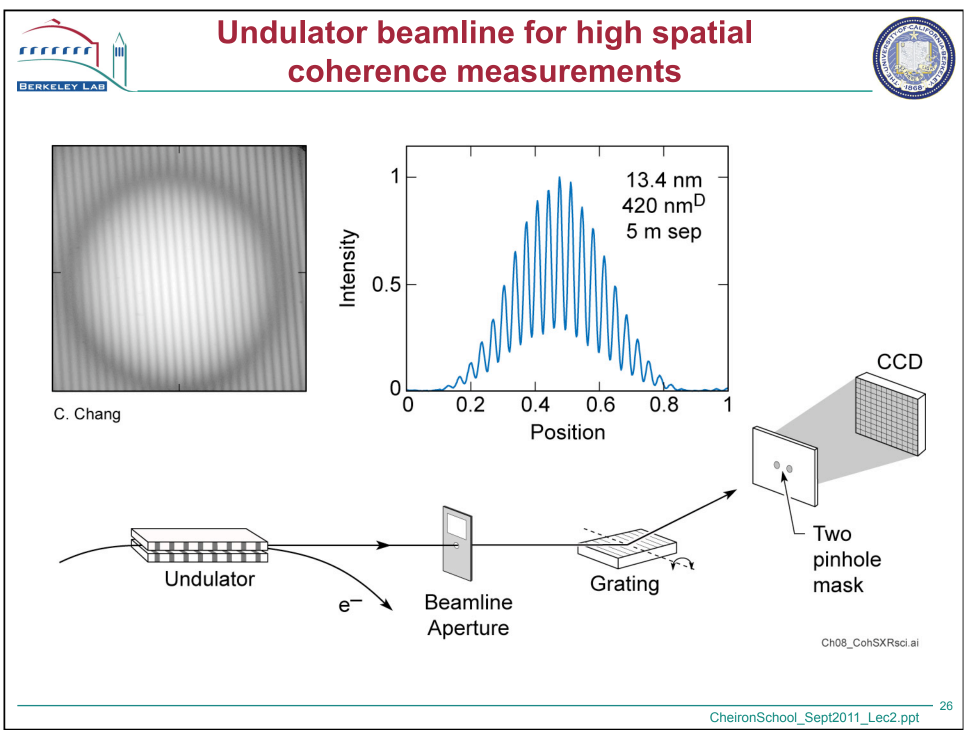
BERKELEY LAB
Undulator beamline for high spatial coherence measurements
C. Chang
13.4 nm
420 nm^D
5 m sep
Intensity
Position
0
0.5
1
0
0.2
0.4
0.6
0.8
1
CCD
Two pinhole mask
Undulator
e⁻
Beamline Aperture
Grating
Ch08_CohSXRsci.ai
26
CheironSchool_Sept2011_Lec2.ppt

Spatial coherence measurements of undulator radiation using the classic 2-pinhole technique

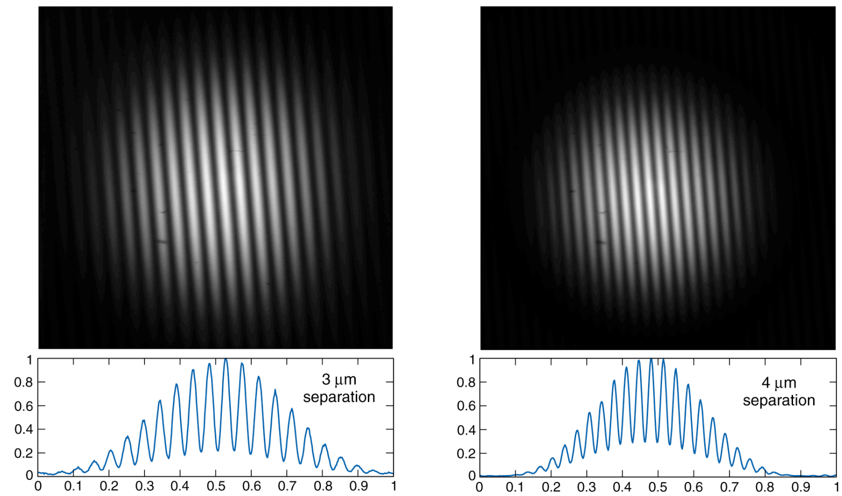

Courtesy of Chang Chang, UC Berkeley and LBNL.

λ = 13.4 nm, 450 nm diameter pinholes, 1024 x 1024 EUV/CCD at 26 cm ALS, 1.9 GeV, λ_u = 8 cm, N = 55

27
CheironSchool_Sept2011_Lec2.ppt

Spatial coherence measurements of undulator radiation using the classic 2-pinhole technique

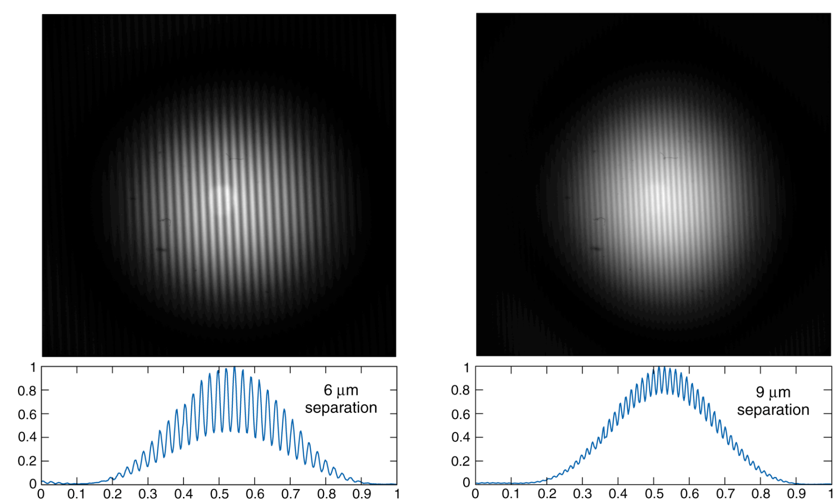

Courtesy of Chang Chang, UC Berkeley and LBNL.

λ = 13.4 nm, 450 nm diameter pinholes, 1024 x 1024 EUV/CCD at 26 cm ALS, 1.9 GeV, λ_u = 8 cm, N = 55

28
CheironSchool_Sept2011_Lec2.ppt

Spatial coherence measurements in the vertical plane

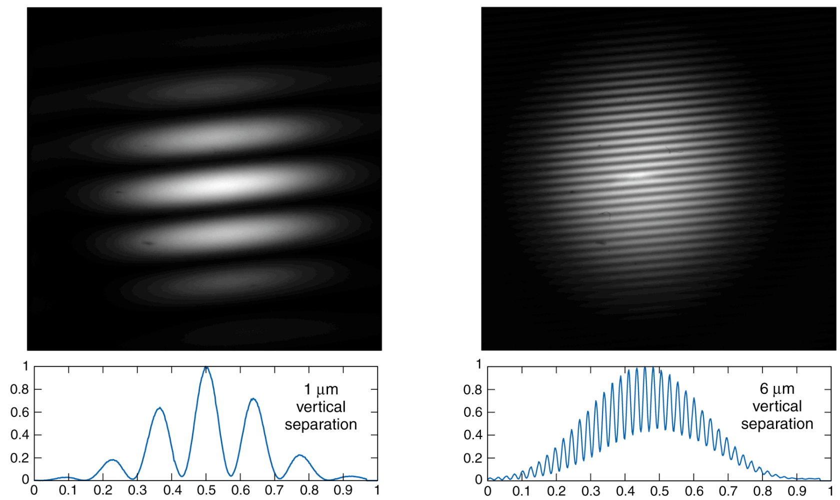

Courtesy of Chang Chang, UC Berkeley and LBNL.

λ = 13.4 nm, 450 nm diameter pinholes, 1024 x 1024 EUV/CCD at 26 cm ALS, 1.9 GeV, λ_u = 8 cm, N = 55

29
CheironSchool_Sept2011_Lec2.ppt

Coherent power for an EPU at the ALS

U5 EPU

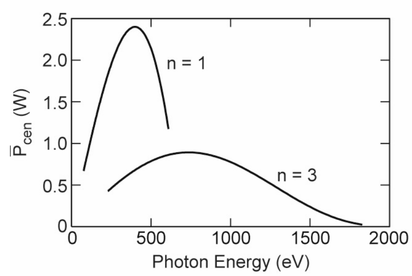

1.9 GeV, 400 mA
λ_u = 50 mm, N = 27
$0.5 \leq K \leq 4.0$
σ_x = 260 μm, σ_x' = 23 μr
σ_y = 16 μm, σ_y' = 3.9 μr
θ_{cen} = 61μr @ K = 0.87 (500 eV)

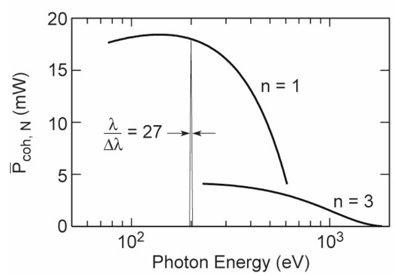

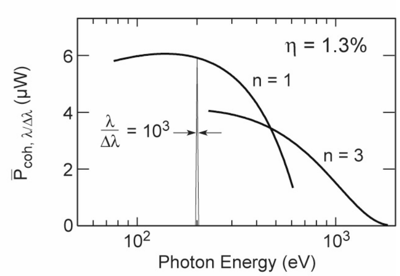

Ch08_ALS_U5epu_Feb07.ai

30
CheironSchool_Sept2011_Lec2.ppt

Coherent power at the Australian Synchrotron

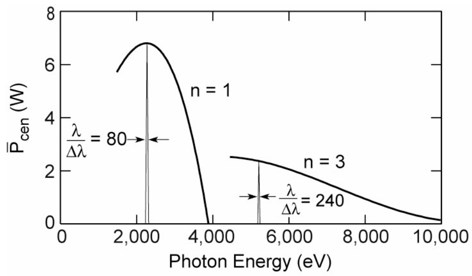

3.0 GeV, 200 mA
λ_u = 22 mm, N = 80
$0 \leq K \leq 1.8$
σ_x = 320 μm, σ_x' = 34 μrad
σ_y = 16 μm, σ_y' = 6 μrad
θ_{cen} = 23 μrad @ K = 1
η = 10%

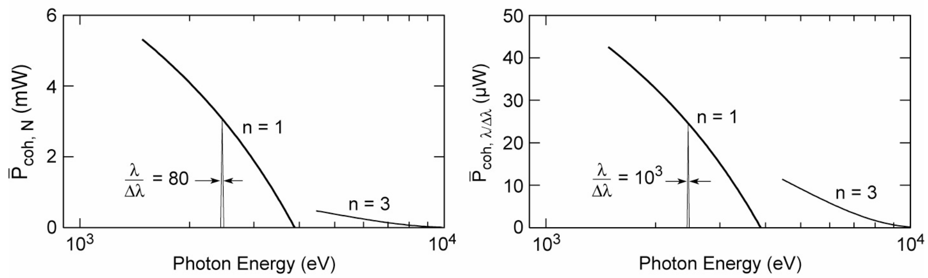

CohPwr_AustralSynch_Feb07.ai

31
CheironSchool_Sept2011_Lec2.ppt

Coherent power at SPring-8

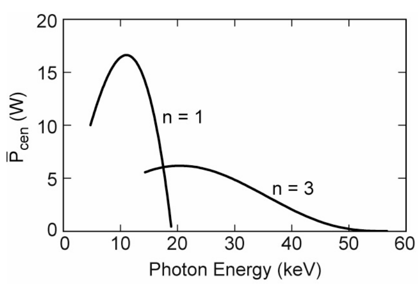

8 GeV, 100 mA
λ_u = 32 mm, N = 140
$0 \leq K \leq 2.46$
σ_x = 393 μm, σ_x' = 15.7 μr
σ_y = 4.98 μm, σ_y' = 1.24 μr
η = 10%

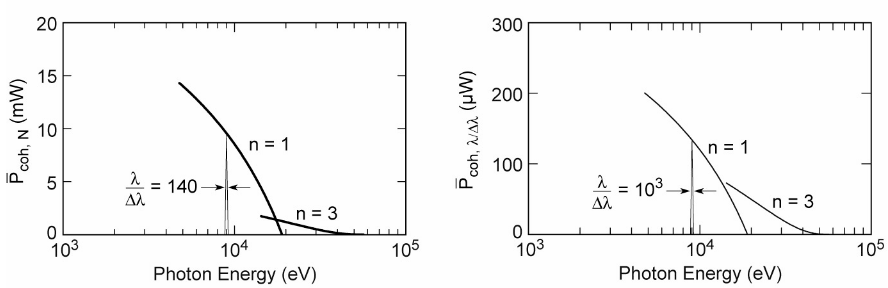

Ch08_SPring8_Feb07.ai

32
CheironSchool_Sept2011_Lec2.ppt

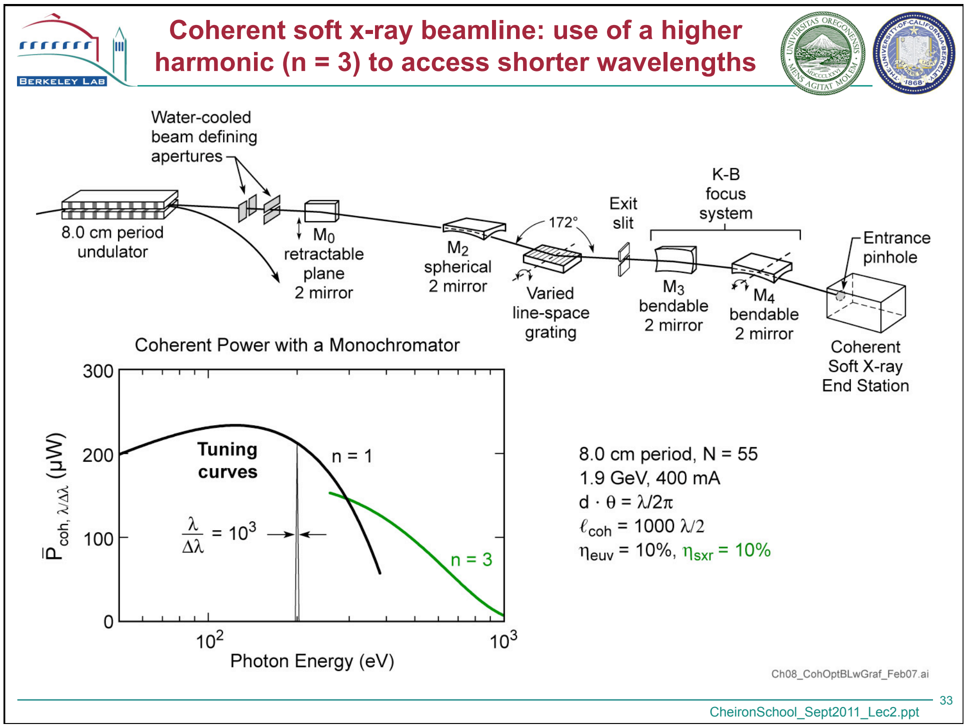
Coherent soft x-ray beamline: use of a higher harmonic (n = 3) to access shorter wavelengths
Water-cooled beam defining apertures
8.0 cm period undulator
M0 retractable plane 2 mirror
M2 spherical 2 mirror
172°
Varied line-space grating
Exit slit
K-B focus system
M3 bendable 2 mirror
M4 bendable 2 mirror
Entrance pinhole
Coherent Soft X-ray End Station
Coherent Power with a Monochromator
300
200
100
0
$\bar{P}_{coh,\ \lambda/\Delta\lambda}$ (μW)
Tuning curves
n = 1
n = 3
$\frac{\lambda}{\Delta\lambda} = 10^3$
10^2
10^3
Photon Energy (eV)
8.0 cm period, N = 55
1.9 GeV, 400 mA
$d \cdot \theta = \lambda/2\pi$
$\ell_{coh} = 1000\ \lambda/2$
η_{euv} = 10%, η_{sxr} = 10%
Ch08_CohOptBLwGraf_Feb07.ai
33
CheironSchool_Sept2011_Lec2.ppt

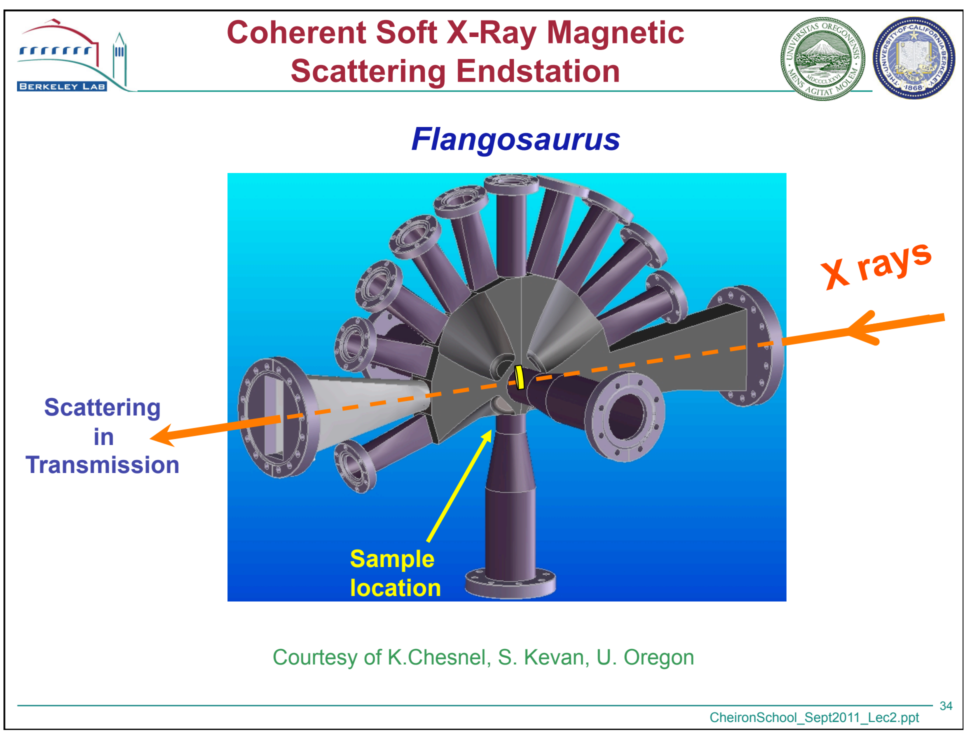
Coherent Soft X-Ray Magnetic Scattering Endstation
Flangosaurus
X rays
Scattering in Transmission
Sample location
Courtesy of K.Chesnel, S. Kevan, U. Oregon
34
CheironSchool_Sept2011_Lec2.ppt

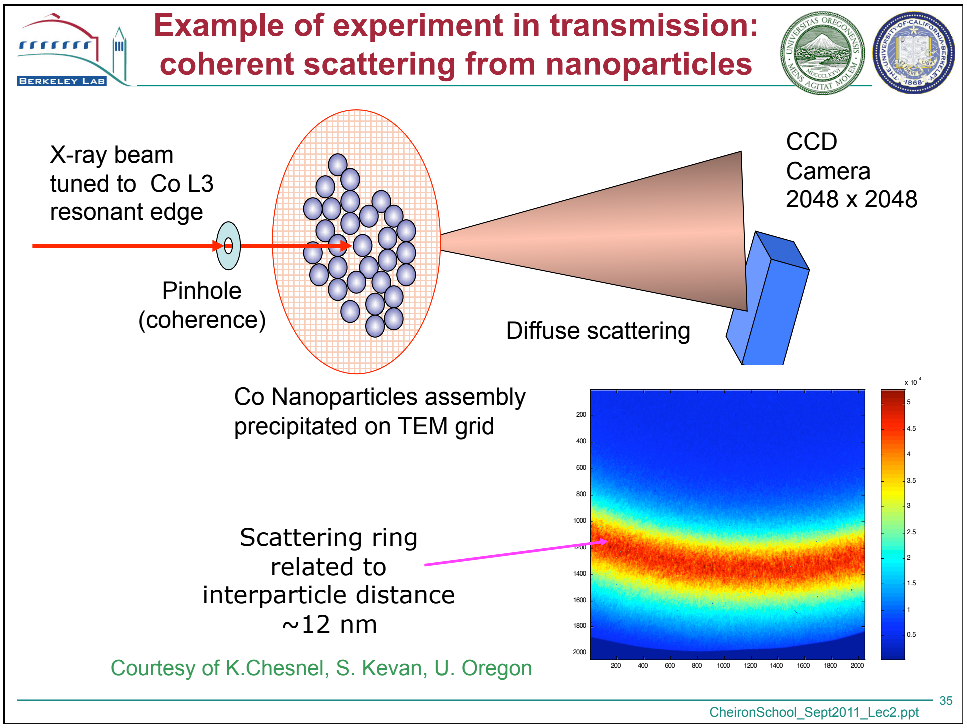
Example of experiment in transmission:
coherent scattering from nanoparticles
X-ray beam
tuned to Co L3
resonant edge
Pinhole
(coherence)
CCD
Camera
2048 x 2048
Diffuse scattering
Co Nanoparticles assembly
precipitated on TEM grid
Scattering ring
related to
interparticle distance
~12 nm
Courtesy of K.Chesnel, S. Kevan, U. Oregon
35
CheironSchool_Sept2011_Lec2.ppt

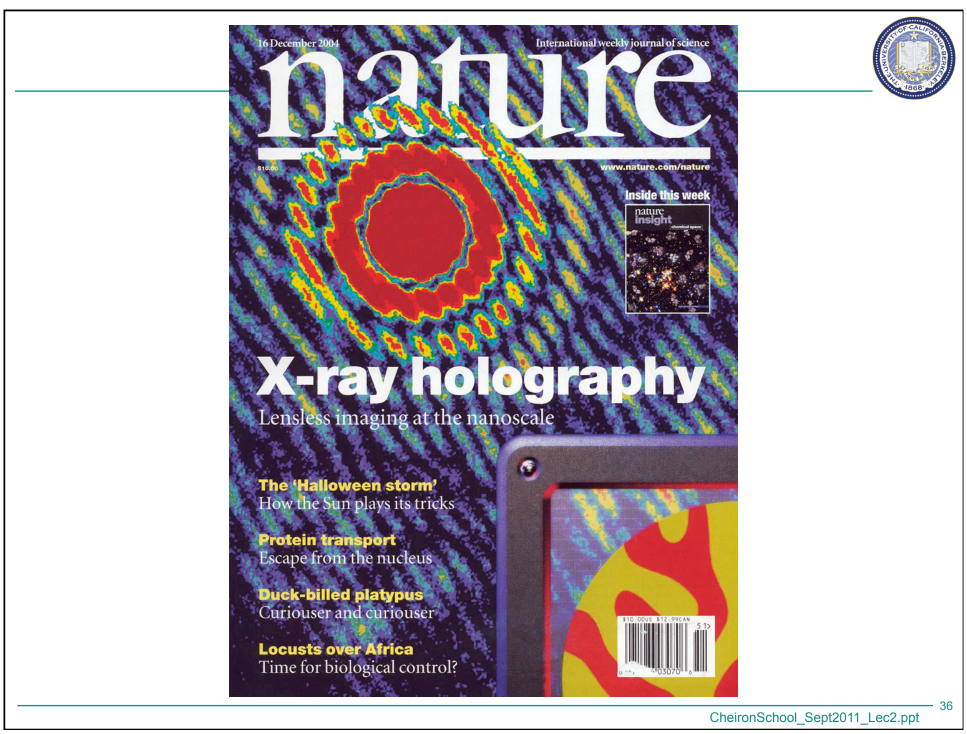
16 December 2004
International weekly journal of science
nature
www.nature.com/nature
Inside this week
X-ray holography
Lensless imaging at the nanoscale
The 'Halloween storm'
How the Sun plays its tricks
Protein transport
Escape from the nucleus
Duck-billed platypus
Curiouser and curiouser
Locusts over Africa
Time for biological control?
36
CheironSchool_Sept2011_Lec2.ppt

Coherent power at BESSY II

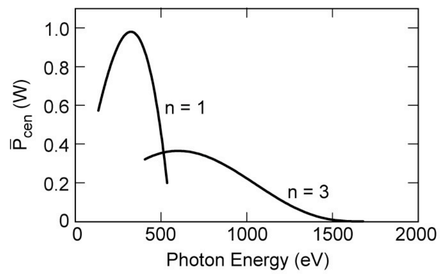

1.7 GeV, 200 mA
λ_u = 49 mm, N = 84
$0 \le K \le 2.5$
σ_x = 314 μm, σ_x' = 18 μr
σ_y = 24 μm, σ_y' = 2 μr
η_{euv} = 10% ; η_{sxr} = 10%

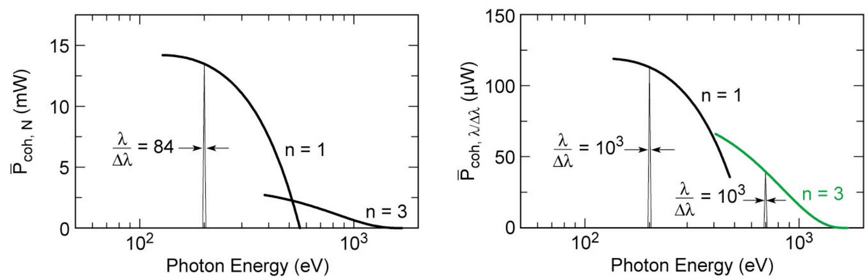

Ch08_BESSYII_Nov07.ai

37
CheironSchool_Sept2011_Lec2.ppt

Lensless imaging of magnetic nanostructures by x-ray spectro-holography

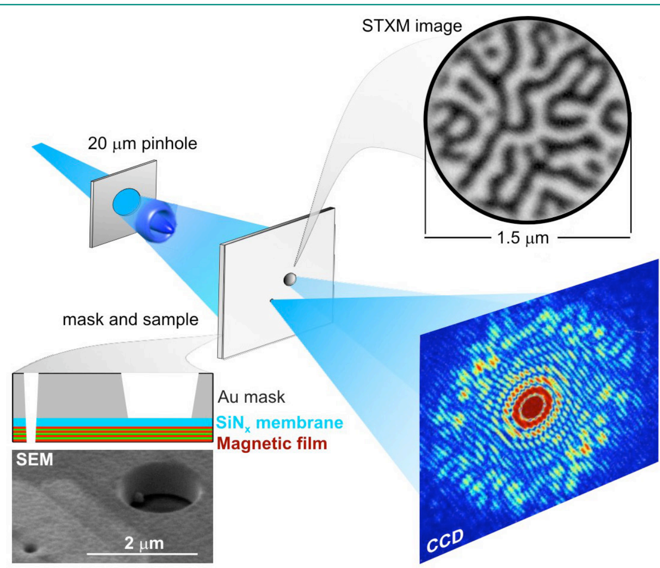

S. Eisebitt, J. Lüning, W.F. Schlotter, M. Lörgen, O. Hellwig,
W. Eberhardt & J. Stöhr / *Nature*, 16 Dec 2004

LenslessImagingF1.ai

38
CheironSchool_Sept2011_Lec2.ppt

Undulators, FELs and coherence

- Spatial coherence
- Temporal coherence
- Partial coherence
- Full coherence
- Spatial filtering
- Uncorrelated emitters
- Correlated emitters
- True phase coherence and mode control
- Lasers, amplified spontaneous emission (ASE) and mode control
- Undulator radiation
- SASE FEL 100^{+} fsec soft/hard x-rays
- Seeded FEL true phase coherent x-rays
- High harmonic generation (HHG) compact fsec/asec EUV
- EUV lasers and laser seeded HHG
- Applications with uncorrelated emitters
- Applications with correlated emitters

UndulatorsFELsCoh.ai

Young's double slit experiment: spatial coherence and the persistence of fringes

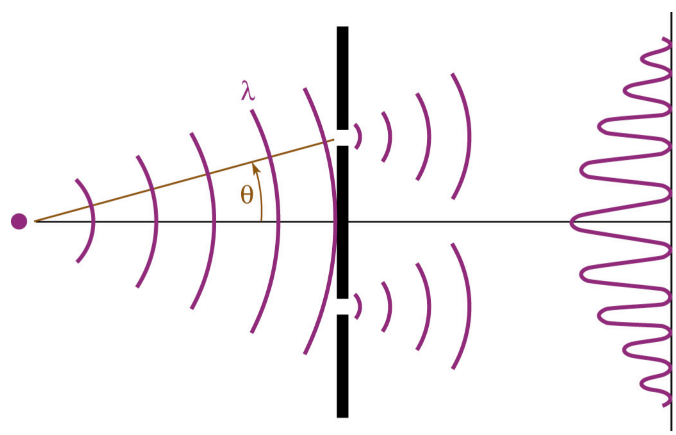

YoungsExprmt.ai

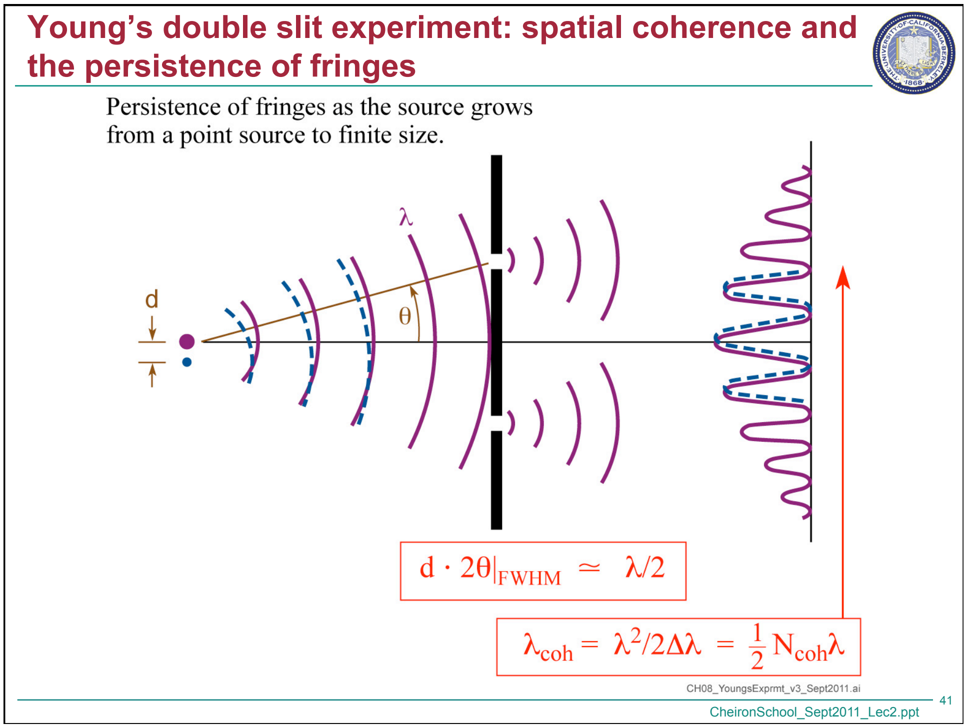
Young's double slit experiment: spatial coherence and the persistence of fringes
Persistence of fringes as the source grows from a point source to finite size.
d
λ
θ
$d \cdot 2\theta|_{FWHM} \simeq \lambda/2$
$\lambda_{coh} = \lambda^2/2\Delta\lambda = \frac{1}{2} N_{coh}\lambda$
CH08_YoungsExprmt_v3_Sept2011.ai
41
CheironSchool_Sept2011_Lec2.ppt

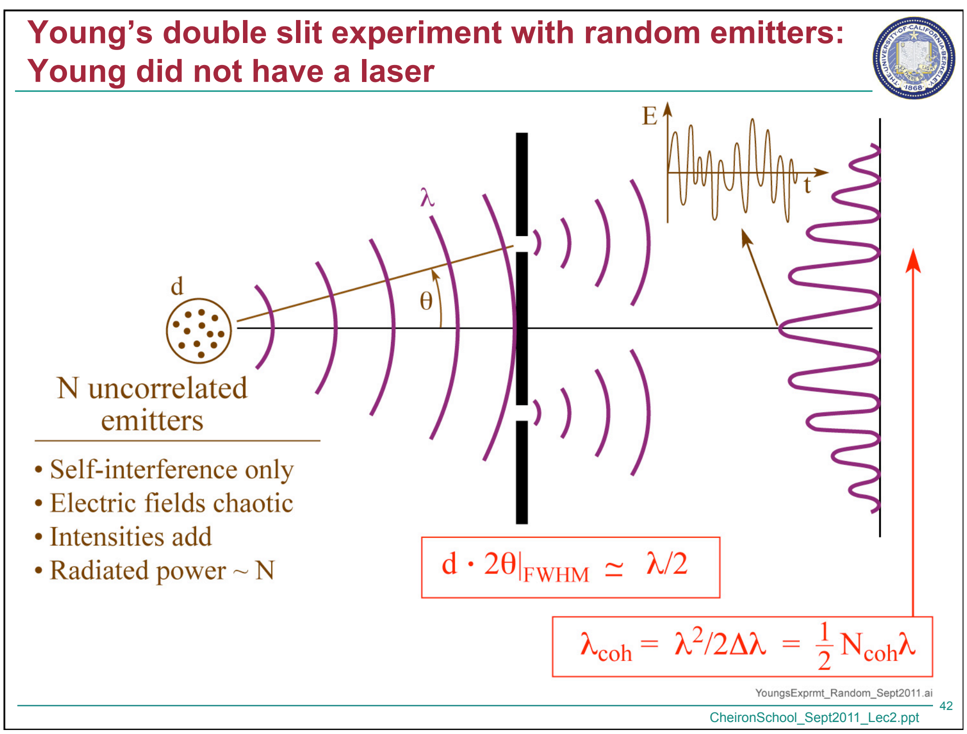
Young's double slit experiment with random emitters: Young did not have a laser
E
t
λ
d
θ
N uncorrelated emitters
• Self-interference only
• Electric fields chaotic
• Intensities add
• Radiated power ~ N
$d \cdot 2\theta|_{FWHM} \simeq \lambda/2$
$\lambda_{coh} = \lambda^2/2\Delta\lambda = \frac{1}{2} N_{coh}\lambda$
YoungsExprmt_Random_Sept2011.ai
42
CheironSchool_Sept2011_Lec2.ppt

Young's double slit experiment with phase coherent emitters (some lasers, or properly seeded FELs)

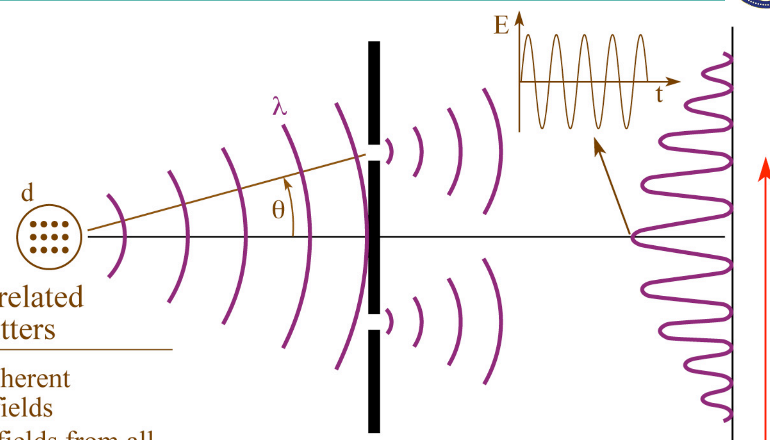

- Phase coherent electric fields
- Electric fields from all particles interfere constructively
- Radiated power ~ N^2
- New phase sensitive probing of matter possible

$$d \cdot 2\theta|_{FWHM} \simeq \lambda/2$$

$$\lambda_{coh} = \lambda^2/2\Delta\lambda = \frac{1}{2} N_{coh}\lambda$$

YoungsExprmt_PhaseCoh_Sept2011.ai

43 CheironSchool_Sept2011_Lec2.ppt

Undulators and FELs

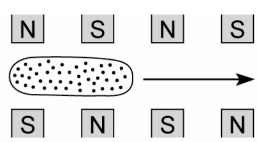

$$\frac{d\mathbf{p}}{dt} = -e(\mathbf{E} + \mathbf{v} \times \mathbf{B})$$

Undulator – uncorrelated electron positions, radiated fields uncorrelated, intensities add, limited coherence, power ~ N.

UndulatorsAndFELs1.ai

44 CheironSchool_Sept2011_Lec2.ppt

Undulators and FELs

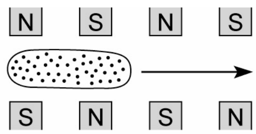

$$\frac{d\mathbf{p}}{dt} = -e(\cancel{\mathbf{E}} + \mathbf{v} \times \mathbf{B})$$

Undulator – uncorrelated electron positions, radiated fields uncorrelated, intensities add, limited coherence, power ~ N.

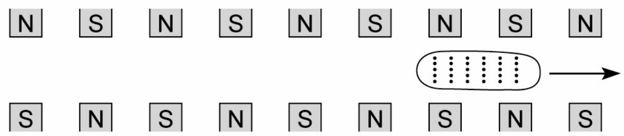

Free Electron Laser (FEL) – very long undulator, electrons are "microbunched" by their own radiated fields into strongly correlated waves of electrons, all radiated electric fields now add, spatially coherent, power ~ N^2

$$\frac{d\mathbf{p}}{dt} = -e(\mathbf{E} + \mathbf{v} \times \mathbf{B})$$

UndulatorsAndFELs2.ai

45

CheironSchool_Sept2011_Lec2.ppt

Undulators and FELs

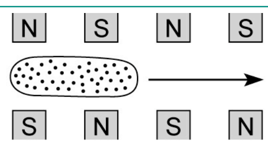

$$\frac{d\mathbf{p}}{dt} = -e(\cancel{\mathbf{E}} + \mathbf{v} \times \mathbf{B})$$

Undulator – uncorrelated electron positions, radiated fields uncorrelated, intensities add, limited coherence, power ~ N.

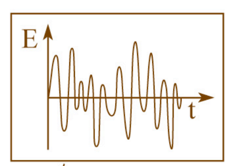

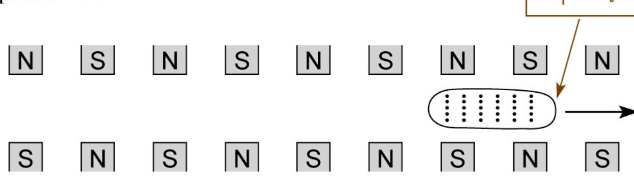

Free Electron Laser (FEL) – very long undulator, electrons are "microbunched" by their own radiated fields into strongly correlated waves of electrons, all radiated electric fields now add, spatially coherent, power ~ N^2

$$\frac{d\mathbf{p}}{dt} = -e(\mathbf{E} + \mathbf{v} \times \mathbf{B})$$

"SASE" FEL – no seed (several separate "waves" of electrons possible with uncorrelated phase.) Less peak power, broader spectrum.

UndulatorsAndFELs2_Sept2011.ai

46

CheironSchool_Sept2011_Lec2.ppt

Seeded FEL

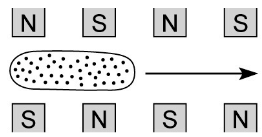

$$\frac{d\mathbf{p}}{dt} = -e(\mathbf{E} + \mathbf{v} \times \mathbf{B})$$

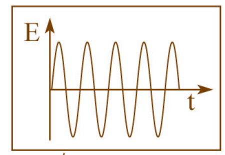

Undulator – uncorrelated electron positions, radiated fields uncorrelated, intensities add, limited coherence, power ~ N.

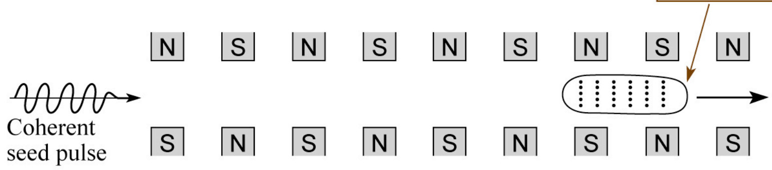

Free Electron Laser (FEL) – very long undulator, electrons are "microbunched" by their own radiated fields into strongly correlated waves of electrons, all radiated electric fields now add, spatially coherent, power ~ N^2

$$\frac{d\mathbf{p}}{dt} = -e(\mathbf{E} + \mathbf{v} \times \mathbf{B})$$

Second generation x-ray FELs.

UndulatorsAndFELs3_Sept2011.ai

47

CheironSchool_Sept2011_Lec2.ppt

FEL Microbunching

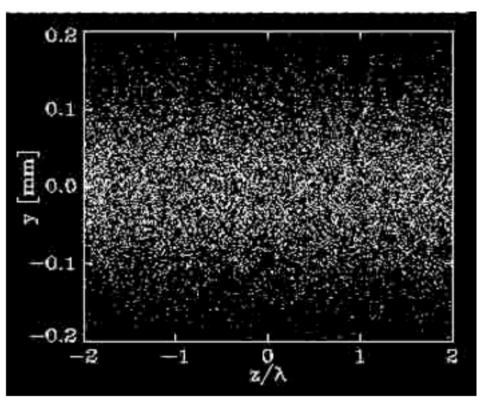

Courtesy of Sven Reiche, UCLA, now SLS

48

CheironSchool_Sept2011_Lec2.ppt

Gain and saturation in an FEL

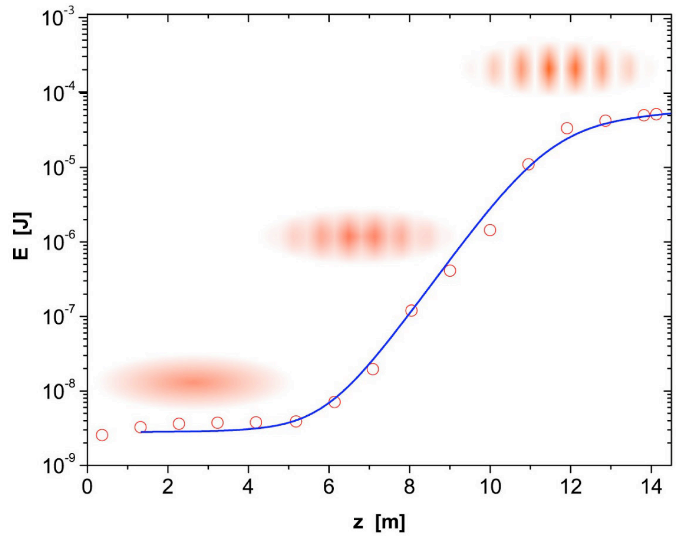

Courtesy of K-J. Kim

Gain_Saturation_FEL_graph.ai

49
CheironSchool_Sept2011_Lec2.ppt

Free electron lasers

Parameters	Flash FEL (Hamburg)	Fermi (Trieste)	LCLS (Stanford, 2010)	SACLA (Harima, 2011)	EU XFEL (Hamburg, 2015)
E_e	230	1.2 GeV	13.6 GeV	8 GeV	17.5 GeV
γ	450/2000	2300	26,600	15,700	35,000
λ_u	27.3 mm	65 mm	30 mm	18 mm	35.6 mm
N	500	216	3700	277	4000
L_u	30 m	14 m	112 m	81 m	200 m
$\hbar\omega$	50-200 eV	30-120 eV	1-10 keV	15 keV	4-12 keV
$\lambda/\Delta\lambda$	100	1000	350	200	1000
$\Delta\tau$	30 fsec	100 fsec	160 fsec	100 fsec	100 fsec
$\dot{\mathcal{F}}$ (ph/pulse)	3×10^{12}	10^{14}	10^{12}	7×10^{11}	10^{14}
rep rate	1 Hz	10 Hz	120 Hz	60 Hz	27 kHz
$\hat{I}$	1.3 kA	500 A	3.4 kA	3 kA	5 kA
$\hat{P}$	0.3 GW	1 GW	8 GW	4 GW	20-100 GW
L	260 m	200 m	5 km	710 m	3.4 km
Polarization	linear	variable	linear	linear	variable
Mode	SASE	Seeded (3ω Ti: saphire)	SASE	SASE	SASE

Flash II, Fermi II, SLS FEL, LCLS II, ...

FreeElectronLasersChart2011.ai

50
CheironSchool_Sept2011_Lec2.ppt

References

1) D. Attwood, *Soft X-Rays and Extreme Ultraviolet Radiation* (Cambridge, UK, 2000); available at Amazon.com.
2) J. Samson and D. Ederer, *Vacuum Ultraviolet Spectroscopy I and II* (Academic Press, San Diego, 1998). Paperback available.
3) J. Als-Nielsen and D. McMorrow, *Elements of Modern X-ray Physics* (Wiley, New York, 2001), 2nd edition (paperback).
4) A. Hofmann, *Synchrotron Radiation* (Cambridge, UK, 2004).

Ch05_ReferencesSept2010.ai

51
CheironSchool_Sept2011_Lec2.ppt

Lectures online at www.youtube.com

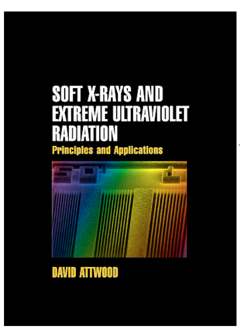

Amazon.com

UC Berkeley
www.coe.berkeley.edu/AST/sxreuv
www.coe.berkeley.edu/AST/srms
www.coe.berkeley.edu/AST/sxr2009

52
CheironSchool_Sept2011_Lec2.ppt